

Online Research @ Cardiff

This is an Open Access document downloaded from ORCA, Cardiff University's institutional repository: <https://orca.cardiff.ac.uk/id/eprint/140990/>

This is the author's version of a work that was submitted to / accepted for publication.

Citation for final published version:

Keatley, Anya C, Dunne, James A, Martin, Tomas L, Nita, Dan C, Andersen, Morten B ORCID: <https://orcid.org/0000-0002-3130-9794>, Scott, Thomas B, Richards, David A and Awbery, Roy P 2021. Uranium isotope variation within vein type uranium ore deposits. *Applied Geochemistry* 131 , 104977. 10.1016/j.apgeochem.2021.104977 file

Publishers page: <https://doi.org/10.1016/j.apgeochem.2021.104977>
<<https://doi.org/10.1016/j.apgeochem.2021.104977>>

Please note:

Changes made as a result of publishing processes such as copy-editing, formatting and page numbers may not be reflected in this version. For the definitive version of this publication, please refer to the published source. You are advised to consult the publisher's version if you wish to cite this paper.

This version is being made available in accordance with publisher policies.

See

<http://orca.cf.ac.uk/policies.html> for usage policies. Copyright and moral rights for publications made available in ORCA are retained by the copyright holders.



Uranium isotope variation within vein type uranium ore deposits

*Anya C. Keatley¹, *James A. Dunne^{2,3}, Tomas L. Martin¹, Dan C. Nita^{3,4}, Morten B. Andersen⁵, Thomas B. Scott¹, David A. Richards³, Roy P. Awbery²*

¹Interface Analysis Centre, School of Physics, University of Bristol, Tyndall Avenue, Bristol, BS8 1TL

²AWE, Aldermaston, Reading, Berkshire, RG7 4PR

³Bristol Isotope Group and School of Geographical Sciences, University of Bristol, University Road, Bristol, BS8 1SS

⁴Institute for Research, Development and Innovation in Applied Natural Sciences, Babeş-Bolyai University, Cluj-Napoca, 400084, Romania

⁵Cardiff University, School of Earth & Ocean Sciences, Main Place, Cardiff, CF10 3AT

*Corresponding author: james.dunne@bristol.ac.uk

Abstract

Isotopic composition of uranium has previously been used to infer the depositional redox environment of uranium ore concentrates and also provide a potential signature to inform nuclear forensic investigations. This study evaluates the diagnostic power of the U isotope signature by investigating the (1) heterogeneity of U isotope compositions in samples collected from the same mine and/or vein, and (2) the influence of U ore processing on $^{238}\text{U}/^{235}\text{U}$ and $^{234}\text{U}/^{238}\text{U}$ ratios. These characteristics are explored via high precision mass spectrometric measurement of vein type uranium ore samples collected predominantly from mines located in central Portugal and South West England. Samples collected from the same vein and mine exhibit $\delta^{238}\text{U}$ values from -0.16 to $+0.03$ (± 0.04) ‰ for and $\delta^{234}\text{U}$ from -1.6 to -64.7 (± 0.4) ‰ for $\delta^{234}\text{U}$ ($\pm 2\text{SD}$). These variations can be attributed to redox-driven isotope fractionation processes and/or U redistribution during localised leaching and re-precipitation. Analyses of residues and leachates from small-scale batch experiments designed to simulate industrial U ore leaching procedures reveal significant positive and negative changes in isotope composition in the leachate relative to the bulk material (up to 0.21 ± 0.06 ‰ for $\delta^{238}\text{U}$ and 62.0 ± 0.6 ‰ for $\delta^{234}\text{U}$). These findings highlight the possibility of significantly different $\delta^{238}\text{U}$ and $\delta^{234}\text{U}$ of uranium ore concentrate from the same mine even if manufacturing processes remain unchanged.

34 **Key Words** – Nuclear Forensics, Uranium, Isotopic fractionation, Uranium ore concentrates

35

36 1 Introduction

37 Nuclear terrorism has been identified as one of the most serious security threats facing the
38 world today (Kristo and Tumey, 2013). As part of the global effort to combat this issue, the
39 International Atomic Energy Agency (IAEA) maintains a database that records incidents of
40 illicit trafficking of nuclear and other radioactive materials (IAEA, 2006). The field of nuclear
41 forensics concerns the analysis of such seized illicit nuclear material to infer details of its
42 production route and origin. For such investigations, the IAEA recommends a suite of
43 analytical tools to detect signatures in intercepted materials (IAEA, 2006), including isotopic
44 analysis, trace elemental impurities, organic impurities, radiochronometry and morphology
45 (Kristo et al. 2016). Here, we focus on the application of high precision uranium isotopic
46 analysis to determine the provenance of uranium ore concentrates (UOCs).

47 Around 40 years ago, significantly anomalous values of the $^{238}\text{U}/^{235}\text{U}$ ratio were reported for
48 uranium (U) ore samples collected from the ~ 2 billion years old natural fission reactors at Oklo
49 and Bangombè in the Republic of Gabon, West Africa (Bodu et al. 1972). Subsequent work
50 found that apart from these nuclear fission reactors, the $^{238}\text{U}/^{235}\text{U}$ was considered to be uniform
51 in natural material with a value of ~ 137.84 (Cowan and Adler, 1976). In the past two decades,
52 high precision analysis of a variety of geological samples has shown that significant $^{238}\text{U}/^{235}\text{U}$
53 variation at the permil-level can occur during U reduction and the exchange between U^{6+} and
54 U^{4+} (Stirling et al. 2007; Abe et al. 2008; Weyer et al. 2008; Heiss et al. 2012; Wang et al.
55 2015). For instance, $^{238}\text{U}/^{235}\text{U}$ offsets of ~ 1 ‰ have been observed between tabular sandstone
56 U deposits and high temperature magmatic deposits. It was suggested that the observed isotopic
57 differences are induced by reduction from U^{6+} to U^{4+} during ore formation at low temperatures
58 and that this fractionation is predominantly a natural expression of the nuclear field shift (Bopp
59 et al., 2009; Brennecka et al., 2010; Lewis et al. 2020). This shift causes ^{235}U to be
60 preferentially incorporated into the dissolved oxidised phase resulting in less ^{235}U in the
61 residual reduced solid (Bigeleisen 1996). Thus, the $^{238}\text{U}/^{235}\text{U}$ fractionation due to nuclear-field
62 shift causes relative enrichment of ^{238}U in the reduced insoluble species (mostly UO_2) and
63 enrichment of ^{235}U in oxidised mobile species such as the uranyl ion, UO_2^{2+} , and its associated
64 aqua complexes. Therefore, these isotope fractionation effects are also expected to be reflected

65 in $^{238}\text{U}/^{235}\text{U}$ ratios in uranium ore minerals formed either by reduction to UO_2 or chemical
66 precipitation in the form of U^{6+} minerals (Uvarova et al. 2014).

67 The mechanism causing natural variation in $^{234}\text{U}/^{238}\text{U}$ isotopic ratios differs from that of the
68 $^{238}\text{U}/^{235}\text{U}$ system. Uranium-234 is an intermediate daughter isotope of ^{238}U decay chain to
69 ^{206}Pb . The ^{238}U decay involves emission of an alpha-particle causing extensive damage to the
70 mineral crystal structure. Consequently, loosely-bound ^{234}U residing in these damaged sites
71 can be preferentially leached or directly recoiled from grain-boundaries during mineral-fluid
72 interactions (Kigoshi, 1971). Variation in $^{234}\text{U}/^{238}\text{U}$ ratios in low temperature environments can
73 vary by over one order of magnitude from open-system conditions (e.g. fluid alteration)
74 showing either enrichment or depletion of ^{234}U depending on the processes of U mobility.
75 However, any $^{234}\text{U}/^{238}\text{U}$ disequilibrium will return to equilibrium within 2.5 Ma by subsequent
76 radioactive decay under closed-system conditions (Ivanovitch, 1992).

77

78 A range of studies have exploited both $^{238}\text{U}/^{235}\text{U}$ and $^{234}\text{U}/^{238}\text{U}$ systematics to infer the
79 geological setting of U ore deposits (e.g. Keegan et al. 2008; Bopp et al. 2009; Brennecka et
80 al. 2010; Uvarova et al. 2014). Brennecka et al. (2010) show that the three main types of U ore
81 deposits (high temperature redox sensitive, low temperature redox sensitive, and non-redox
82 sensitive) all exhibit significantly different $^{238}\text{U}/^{235}\text{U}$ values. Subsequent studies, including the
83 analysis of further deposit types, indicated a range of 1.8 ‰ for $^{238}\text{U}/^{235}\text{U}$ (Uvarova et al. 2014).
84 Uranium isotopic ratios are now routinely used in nuclear forensics investigation. For example,
85 when a green radioactive powder was seized in Australia, the $^{234}\text{U}/^{238}\text{U}$, $^{235}\text{U}/^{238}\text{U}$ and $^{236}\text{U}/^{238}\text{U}$
86 signatures of the material were found to be consistent with UOCs from the Mary Kathleen mine
87 (Keegan et al. 2014). Similarly, the $^{234}\text{U}/^{238}\text{U}$ value of samples taken from three active
88 Australian mines (Ranger, Olympic Dam and Beverly) were found to be significantly different
89 and could be used as a tool to distinguish UOC taken from each of these sites (Keegan et al.
90 2008). In summary, previous work has shown that $^{238}\text{U}/^{235}\text{U}$ can be utilised to infer the
91 depositional setting of a U ore, therefore the $^{238}\text{U}/^{235}\text{U}$ signature can potentially be used
92 predictively. However, the $^{234}\text{U}/^{238}\text{U}$ signature is expected to be site-specific because it is
93 controlled by fluid-mediated transport, which is affected by the permeability, mineralogy and
94 geological structure of each mineral deposit and bounding lithologies.

95

96 Although the $^{238}\text{U}/^{235}\text{U}$ signature has been used to infer U ore deposit type (Bopp et al., 2009;
97 Brennecka et al., 2010), work by Chernyshev et al. (2014) showed significant variation, not

98 only for minerals from individual deposits (up to 0.7 ‰), but also within single pitchblende
99 crystals, with early growth zones enriched in ^{238}U relative the latest growth zones (Chernyshev
100 et al., 2014). It is evident that U isotopic composition varies significantly between U ores of
101 different deposit types, however, few studies have focused on the variation of this signature for
102 samples collected from the same mine (e.g. Kirchenbauer et al. 2016). Uranium isotopic
103 heterogeneity such as this could potentially mislead nuclear forensic studies that utilise U
104 isotope ratios as key classifying features to distinguish between different types of UOC. For
105 example, different batches of a “characterised” UOC may be produced using U ore from
106 different extraction events. Localised U isotope heterogeneity may therefore cause different
107 batches of UOC (from the same UOC producer) to yield an inconsistent U isotopic
108 composition.

109

110 Furthermore, the effect of processing on the isotopic signatures of U ore has not been
111 thoroughly tested. During processing, mined ore is crushed and pulverised to maximise the
112 liberation of U during leaching. Depending on the deposit type and mineralogy of the ore, the
113 size fraction may vary from 5 to 0.074 mm (IAEA, 1993). Leaching is generally carried out by
114 the addition of sulphuric acid (low cost and widely available) with an oxidant (usually ferric
115 iron oxide) to convert the insoluble U^{4+} to soluble U^{6+} (IAEA, 1993). Laboratory experiments
116 have shown that during the oxidation of U^{4+} in HCl media in the presence of dissolved oxygen,
117 the $^{238}\text{U}/^{235}\text{U}$ value of the remaining U^{4+} increased with time, while the $^{238}\text{U}/^{235}\text{U}$ of the U^{6+}
118 product decreased (Wang et al., 2015). In addition, Stirling et al. (2007) conducted a series of
119 sequential acid leaching experiments with single crystals of uraninite and euxenite (with
120 radiation-damaged areas). The results indicated that mineral weathering is a possible
121 mechanism by which ^{235}U can be fractionated from ^{238}U in ground waters (Stirling et al., 2007).
122 Therefore, if fractionation has been observed in the natural environment and under laboratory
123 conditions at short timescales, it is possible that processing U ore by acid leaching, which
124 involves the transition from U^{4+} to U^{6+} , could also cause fractionation of the $^{234}\text{U}/^{238}\text{U}$ and
125 $^{238}\text{U}/^{235}\text{U}$ ratios. If the extent of isotopic fractionation is inconsistent during conversion of
126 uranium ore to UOC, one can expect UOCs from the same mine and processing to yield an
127 inconsistent uranium isotope signature.

128

129 To explore potential changes in U isotopic composition in U ores and processed materials, we
130 apply high-precision multi-collector inductively coupled plasma mass spectrometry (MC-
131 ICPMS) U isotope measurement techniques to a suite of 42 vein type U ores from different

132 mines, districts and regions in Portugal and South West (SW) England. Isotopic analyses of
 133 these samples are expected to build upon the previous work by Keatley et al. (2015, 2016),
 134 which focused on mineralogical and chemical data. These data are supplemented by sites
 135 situated in Niger, Namibia, Zambia and Australia. Where possible, suitable U ore samples were
 136 collected using a hierarchical approach: along the same mineral vein, within the same mine and
 137 for different mines within the region influenced by granite intrusion. A subset of the samples
 138 was leached, following industrial protocols as closely as possible at the laboratory scale, to
 139 examine changes in the isotopic composition of U during processing. The $^{238}\text{U}/^{235}\text{U}$ and
 140 $^{234}\text{U}/^{238}\text{U}$ values of the initial ore and the resulting leachate were measured to monitor for
 141 changes caused by the leaching process. All the values here are given in the form of $\delta^{238}\text{U}$ and
 142 $\delta^{234}\text{U}$, which are calculated as follows:

143

$$144 \quad \delta^{238}\text{U} = \left[\frac{\left(\frac{^{238}\text{U}}{^{235}\text{U}} \right)_{\text{sample}}}{\left(\frac{^{238}\text{U}}{^{235}\text{U}} \right)_{\text{standard}}} - 1 \right] \times 1000$$

145

$$146 \quad \delta^{234}\text{U} = \left[\frac{\left(\frac{^{234}\text{U}}{^{238}\text{U}} \right)_{\text{sample}}}{\left(\frac{^{234}\text{U}}{^{238}\text{U}} \right)_{\text{sec.equilib.}}} - 1 \right] \times 1000$$

147

148 For $\delta^{238}\text{U}$, the standard is CRM112A with the $^{235}\text{U}/^{238}\text{U}$ value equal to 137.829 (Hiess et al.
 149 2012). For $\delta^{234}\text{U}$, the secular equilibrium value for $^{234}\text{U}/^{238}\text{U}$ is 5.491×10^{-5} (Cheng et al. 2013).

150 2 Materials & Methods

151

152 2.1 Sample collection and preparation

153 Most of the U ores analysed in this study were collected from the Beiras region of Portugal and
 154 SW England, UK, with other samples from Australia, Namibia, Zambia and Niger. The Beiras
 155 region is situated in central Portugal, where hydrothermal mineral veins within the Hercynian
 156 Granites (intruded ~ 290 Ma) were mined throughout the 20th century. The region has four
 157 distinct uranium provinces (Cameron 1982a), three of which were sampled in this study; spoil
 158 heaps at eight disused mine sites from the Guarda province to the east, Roboleiro province to
 159 the north and the Urgeiriça province to the west (Cameron 1982b).

160

161 For SW England, samples were collected from 14 different mines where U mineralisation has
162 been documented. Most of these samples were collected from spoil heaps. However, to
163 examine isotopic heterogeneity for samples collected from within the same mine and/or the
164 same vein, samples were taken *in situ* at Kingswood and Carbis Bay mines (Keatley et al.
165 2015). These samples were extracted along major zones of mineralisation in veins of the
166 respective mines by mechanical trepanning using a hand-held drill fitted with 14-mm diamond
167 core drill bit. Between drilling, samples and core pieces were cleaned thoroughly to avoid cross
168 contamination. Prior to dissolution, all samples were crushed and sieved to generate a
169 homogenised fine powder ($< 63 \mu\text{m}$).

170

171 2.2 Sample dissolution, spiking and, column chemistry

172 Prior to dissolution, the ^{233}U - ^{236}U spike IRMM-3636 was added, aiming for a $^{238}\text{U}/^{236}\text{U}$ of
173 ~ 150 . The sample was subsequently dissolved in a mixture of concentrated HF/HNO₃/HCl
174 acid, dried and treated with concentrated HNO₃ and H₂O₂ to oxidise residual organics. Uranium
175 was separated from all other matrices using a UTEVA column procedure as reported in
176 Andersen et al. (2014). In brief, the sample was dissolved in 3 ml of 3 mol/L HNO₃ and loaded
177 onto 1 ml of UTEVA resin (Eichrom) in Teflon columns precleaned in 9 ml 0.1 mol/L HCl –
178 0.3 mol/L HF, 5 ml 18 MΩcm water and preconditioned in 7 ml 3 mol/L HNO₃. Matrix
179 elements were eluted with 7 ml 3 mol/L HNO₃ followed by 3 ml 3 mol/L HCl and U collected
180 by loading 8 ml 0.1 mol/L HCl + 0.3 mol/L HF. Samples were dried down and fluxed in
181 concentrated HNO₃ + H₂O₂ to eliminate organics introduced during column chemistry. For
182 measurement by MC-ICPMS, the samples were redissolved in 0.6 mol/L HCl and adjusted to
183 a ^{238}U concentration of $\sim 500 \mu\text{g/L}$. Uranium recoveries of $> 95 \%$ were achieved via this
184 method with total chemistry U blanks of $< 20 \text{ ng}$.

185

186 2.3 MC-ICPMS instrument set-up

187 Uranium isotope ratio measurements were performed using a Thermo Finnigan Neptune MC-
188 ICPMS at the University of Bristol Isotope Group facilities, equipped with a standard sample
189 and X-skimmer cone. The instrument was operated in low mass resolution ($M/\Delta M \approx 450$) using
190 an Aridus desolvating nebuliser introduction system. These conditions typically yielded U⁺
191 transmission efficiencies of $\sim 1.5 \%$. All measurements were made in static mode using the
192 configuration described in Andersen et al. (2014, 2015). To set-up for $^{238}\text{U}^+$ beam intensities
193 $> 500 \text{ pA}$, the ^{238}U cup was connected to a feedback amplifier with a $10^{10} \Omega$ resistor, instead

194 of the conventional $10^{11} \Omega$ feedback amplifier resistors. A $10^{12} \Omega$ resistor was used for lower
195 intensity ^{234}U beam. All other cups were connected to feedback amplifiers with $10^{11} \Omega$ resistors.
196 Typical ion beam intensities were $^{238}\text{U} \approx 400 \text{ V}$, $^{235}\text{U} \approx 3 \text{ V}$, $^{234}\text{U} \approx 20 \text{ mV}$ and $^{233, 236}\text{U} \approx 2 \text{ V}$
197 (voltages normalised to a $10^{11} \Omega$ resistor). These signals were integrated over a period of 80 x
198 4 s, while background intensities prior to measurements remained $< 20 \text{ ppm}$ of the total $^{238}\text{U}^+$
199 sample beam. Sample measurements were bracketed individually and normalised to
200 measurements of CRM-112A spiked with IRMM-3636. Tailing and hydrides were monitored
201 and corrected for where necessary as described in Andersen et al. (2014). Hydride formation
202 and high-mass tailing (m/z 239.05/ ^{238}U) and the abundance sensitivity (m/z 237.05/ ^{238}U)
203 remained stable through measurement sequences at $\sim 2 - 3 \times 10^{-6}$. Adequate separation of Th
204 from U eliminated the requirement to correct for $^{232}\text{ThH}^+$ and 1 a.m.u. high mass tailing of
205 ^{232}Th on ^{233}U . Mass bias corrections were performed using the exponential mass fractionation
206 law (Russell et al. 1978). Corrections were also made to account for ^{234}U , ^{235}U , ^{238}U impurities
207 in IRMM-3636 (see Andersen et al. 2015 for further details).

208

209 During the measurement sessions internal measurement errors ($\pm 2\text{SE}$) for $\delta^{238}\text{U}$ were < 0.03
210 ‰ and $< 0.4 \text{ ‰}$ for $\delta^{234}\text{U}$ (improved precision using the $10^{12} \Omega$ resistor for the ^{234}U beam). Of
211 the measured samples, 69 were measured two or three times. Of these, 63 samples reproduced
212 within $\pm 0.03 \text{ ‰}$ for the $\delta^{238}\text{U}$ and all the samples were within $\pm 0.4 \text{ ‰}$ for $\delta^{234}\text{U}$. The largest
213 difference for two duplicated $\delta^{238}\text{U}$ measurements was 0.09 ‰ (see Supplementary Material).
214 Detailed measurement performance using this specific set-up is described in Andersen et al.
215 (2015). Repeated standard measurements of the standards BHVO-2 ($\delta^{238}\text{U} = -0.314 \pm 0.028$
216 ‰, 2SD) and inhouse CZ-1 uraninite ($\delta^{238}\text{U} = -0.053 \pm 0.029 \text{ ‰}$, 2SD) gave overall external
217 reproducibility of $\pm 0.03\text{‰}$ per individual analysis and good agreement with previously
218 reported values for both standards. The external reproducibility of $\delta^{234}\text{U}$ are limited by low
219 ^{234}U intensities ($< 0.2 \text{ pA}$) but were $< 3 \text{ ‰}$ (2 SD) for the standards and in agreement with
220 previously reported values (Andersen et al. 2015).

221

222 To further test the accuracy of this method, a sub-set of the ten processed samples were also
223 measured on a Nu Instruments Nu Plasma II MC-ICP-MS using a Aridus II desolvating
224 nebulizer system at CELTIC, Cardiff University. The U isotope measurements were conducted
225 in 0.3 mol/L HNO_3 at low mass resolution ($M/\Delta M \sim 400$), collected in static mode with all the
226 isotopes of interest (^{232}Th , ^{233}U , ^{234}U , ^{235}U , ^{236}U , ^{238}U) in Faraday cups fitted with $10^{11} \Omega$

227 resistors, following the set-up in Stirling et al. (2007). General U transmission efficiencies were
228 ~ 1 % and measurements were conducted using typical ^{238}U ion beams of $\sim 4 \times 10^{-10}$ amps with
229 data integration over a 60 x 5 s periods, with an 0.3 mol/L HNO_3 on-peak blank measurement,
230 subtracted from the succeeding sample measurement. Data correction and standard
231 normalisation were similar as reported above. The internal precisions on measured $\delta^{238}\text{U}$ values
232 are better than ± 0.05 ‰ (2SE) for all samples. The external reproducibility of $\delta^{238}\text{U}$ for the in-
233 house CZ-1 gave $\delta^{238}\text{U}$ of -0.03 ± 0.06 ‰ and -2 ± 10 ‰ for the low precision $\delta^{234}\text{U}$
234 measurements (2 SD, n=6) in good agreement with above measurements of the same standard
235 at University of Bristol. For the $\delta^{238}\text{U}$, nine out of the ten replicate measurements were
236 reproduced within 0.06 ‰ (one sample showing 0.10‰ difference), and all the $\delta^{234}\text{U}$ were
237 within 10 ‰ when compared to the high-precision measurements (see Supplementary
238 Material). Based on these tests for reproducibility and accuracy, a conservative estimate of
239 ± 0.04 ‰ for $\delta^{238}\text{U}$ and ± 0.4 ‰ for $\delta^{234}\text{U}$ (2SD) have been used for all the data reported in the
240 following.

241

242 2.4 Leaching experiments

243 Details of industry practices for the leaching of vein type U ores were reviewed and the
244 following experiment was designed to mimic protocols as closely as possible (Kristo et al.
245 2016). Uranium ore samples were ground and sieved to < 75 μm , 1 g of ore was leached in 250
246 ml of 0.015 mol/L (pH = 2) H_2SO_4 . No additional oxidant was added but the solution was
247 constantly agitated by a magnetic stirrer to promote ingress of atmospheric oxygen. Aliquots
248 (5 ml) of the leachate were taken at 0.5, 1, 2, 3, 4, 5, 7, 10, 15 and 24 hours. At each leachate
249 sampling step, temperature, pH, dissolved oxygen, conductivity, and redox potential were
250 measured. Each aliquot was filtered using a 0.33 μm Millipore Express Millex GP filter and
251 dried prior to separation chemistry. A total of 42 U ore samples were analysed for bulk U
252 isotopic ratios. Of these U ore samples, isotopic measurements were performed on 17 samples
253 following a 24-hr acid leach experiment, four samples after a 0.5-hr acid leach and seven acid-
254 leach residues.

255

256 3 Results

257

258 3.1 Bulk samples

259 Measurements of bulk U ore samples exhibit a large range of $\delta^{238}\text{U}$ and $\delta^{234}\text{U}$ values. Of the
 260 42 samples analysed (Table 1), the lowest observed $\delta^{238}\text{U}$ value ($-0.63 \pm 0.04 \text{ ‰}$) was from a
 261 torbernite ore (Guarda region of Portugal). The highest $\delta^{238}\text{U}$ value of $0.15 \pm 0.04 \text{ ‰}$ was found
 262 in a pitchblende sample (Niger). For $\delta^{234}\text{U}$, the most ^{234}U depleted sample ($\delta^{234}\text{U} = -154.6 \pm$
 263 0.4 ‰) was a metatyuyamunite (Littleham Cove mine, Dartmoor, England), while the most
 264 ^{234}U enriched sample ($\delta^{234}\text{U} = 186.8 \pm 0.4 \text{ ‰}$) was a tobernite ore (Reboleiro, Portugal).

265 *Table 1: Sample information and U isotopic data for ore samples from a range of different*
 266 *geochemical settings, mines and veins (see supplementary material for further details on the*
 267 *uncertainties). The redox state is provided for those samples included in redox comparisons*
 268 *performed in the subsequent text.*

Sample ID	Mine	Granite	Country	Uranium Mineralogy	Redox state	$\delta^{238}\text{U}$	$\pm 2\text{SD}$	$\delta^{234}\text{U}$	$\pm 2\text{SD}$
MAY_7	Botallack	Lands End	England	Bijvoetite-Y + coffinite	Reduced	-0.279	0.040	-7.5	0.4
BOT2	Botallack	Lands End	England	Uraninite, Bijvoetite-Y + coffinite	Reduced	0.050	0.040	0.9	0.4
KCB5	Carbis Bay	Lands End	England	Torbernite, Zeunerite	Oxidised	0.032	0.040	-30.6	0.4
CBJ1	Carbis Bay	Lands End	England	Torbernite, RRUP, Zeunerite		-0.330	0.040	-8.0	0.4
KCB1	Carbis Bay	Lands End	England	Torbernite, Zeunerite		-0.158	0.040	-6.6	0.4
CBJ6	Carbis Bay	Lands End	England	Torbernite	Oxidised	-0.321	0.040	24.9	0.4
KW12	Kingswood Adit	Dartmoor	England	W- Bi- Uraninite, Zeunerite, Zeunerite +W		-0.289	0.040	-64.7	0.4
KW10	Kingswood Adit	Dartmoor	England	Zeunerite		-0.175	0.040	-36.7	0.4
KW4	Kingswood Adit	Dartmoor	England	W- Uraninite, Threadgoldite, Chistyakovite, Autunite		-0.210	0.040	-1.6	0.4
LV2	Levant	Lands End	England	Bijvoetite-Y + coffinite	Reduced	-0.05	0.040	4.9	0.4
L2	Littleham Cove	Dartmoor	England	Metatyuyamunite		-0.018	0.040	-154.6	0.4
B2	Polwheveral Creek	Carmenellis	England	Iron oxide + U		0.113	0.040	-113.2	0.4
S107	Site 1	Guarda	Portugal	Torbernite	Oxidised	-0.632	0.040	-9.0	0.4
S109	Site 1	Guarda	Portugal	Saleeite, Bassetite	Oxidised	-0.070	0.040	7.5	0.4
S108	Site 1	Guarda	Portugal	Torbernite	Oxidised	0.152	0.040	-0.3	0.4
S221	Site 2	Roboleiro	Portugal	Torbernite	Oxidised	0.147	0.040	10.4	0.4
S206	Site 2	Roboleiro	Portugal	Torbernite	Oxidised	0.099	0.040	-2.5	0.4
S301	Site 3	Roboleiro	Portugal	Torbernite		-0.164	0.040	6.6	0.4
S403	Site 4	Roboleiro	Portugal	Torbernite, Zeunerite	Oxidised	-0.448	0.040	65.8	0.4
S404	Site 4	Roboleiro	Portugal	Torbernite	Oxidised	-0.302	0.040	5.0	0.4
S502	Site 5	Roboleiro	Portugal	Autunite	Oxidised	-0.217	0.040	27.8	0.4
S606	Site 6	Roboleiro	Portugal	Autunite	Oxidised	-0.472	0.040	-2.7	0.4
S601	Site 6	Roboleiro	Portugal	Phosphuranylite	Oxidised	-0.425	0.040	-3.0	0.4
S602	Site 6	Roboleiro	Portugal	Torbernite	Oxidised	-0.465	0.040	186.8	0.4
S701	Site 7	Urgeiriça	Portugal	Autunite	Oxidised	-0.305	0.040	0.0	0.4
S802	Site 8	Urgeiriça	Portugal	Autunite	Oxidised	-0.409	0.040	40.8	0.4
S804	Site 8	Urgeiriça	Portugal	Autunite	Oxidised	-0.469	0.040	26.8	0.4
S803	Site 8	Urgeiriça	Portugal	Autunite	Oxidised	-0.159	0.040	-8.5	0.4
S805	Site 8	Urgeiriça	Portugal	Autunite	Oxidised	-0.073	0.040	-10.4	0.4
STMA1	South Terras	St Austell	England	Torbernite	Oxidised	-0.145	0.040	-4.6	0.4
SAC9	St Austell Consols	St Austell	England	Pb-W-Uraninite	Reduced	0.06	0.040	1.0	0.4
WC1	Wheal Cock	Lands End	England	Bijvoetite-Y + coffinite, Coffinite	Reduced	-0.175	0.040	-9.3	0.4
LED4	Wheal Edward	Lands End	England	Torbernite, Zeunerite	Oxidised	-0.144	0.040	-0.01	0.4
OWA1	Wheal Owles	Lands End	England	Cuprosklodowskite, Uranophane	Oxidised	-0.214	0.040	35.0	0.4
OW2	Wheal Owles	Lands End	England	Bijvoetite-Y + coffinite, Uraninite, Uranophane, Coffinite		-0.52	0.040	2.0	0.4
TW1	Wheal Trenwith	Lands End	England	Pb-W-Uraninite, Torbernite, Uraninite, Zeunerite		-0.107	0.040	-99.9	0.4

WT1	Wheal Trewavas	Tregonning-Godolphin	England	Torbernite	Oxidised	-0.364	0.040	16.3	0.4
OREAS 106	-	-	Australia	-		-0.337	0.040	-8.0	0.4
Namibia	-	-	Namibia	Carnotite + Si	Oxidised	-0.458	0.040	1.5	0.4
Zambia	-	-	Zambia	Pb - Uraninite	Reduced	-0.227	0.040	0.9	0.4
Niger1	Niger 1	-	Niger	Pitchblende	Reduced	0.131	0.040	39.4	0.4
Niger2	Niger 2	-	Niger	Pitchblende	Reduced	0.293	0.040	-147.4	0.4

269

270

271 3.2 Changes in U isotope composition caused by acid leaching

272 Following a 24-hr leach in dilute sulphuric acid, we determined the difference in isotopic
 273 composition observed in the leachate relative to original bulk material (Table 2). We report this
 274 as $\Delta^{238}\text{U}_{\text{leach-bulk}}$ and $\Delta^{234}\text{U}_{\text{leach-bulk}}$:

$$275 \Delta^{23x}\text{U}_{\text{leach-bulk}} = \delta^{23x}\text{U}_{\text{leach}} - \delta^{23x}\text{U}_{\text{bulk}}$$

276

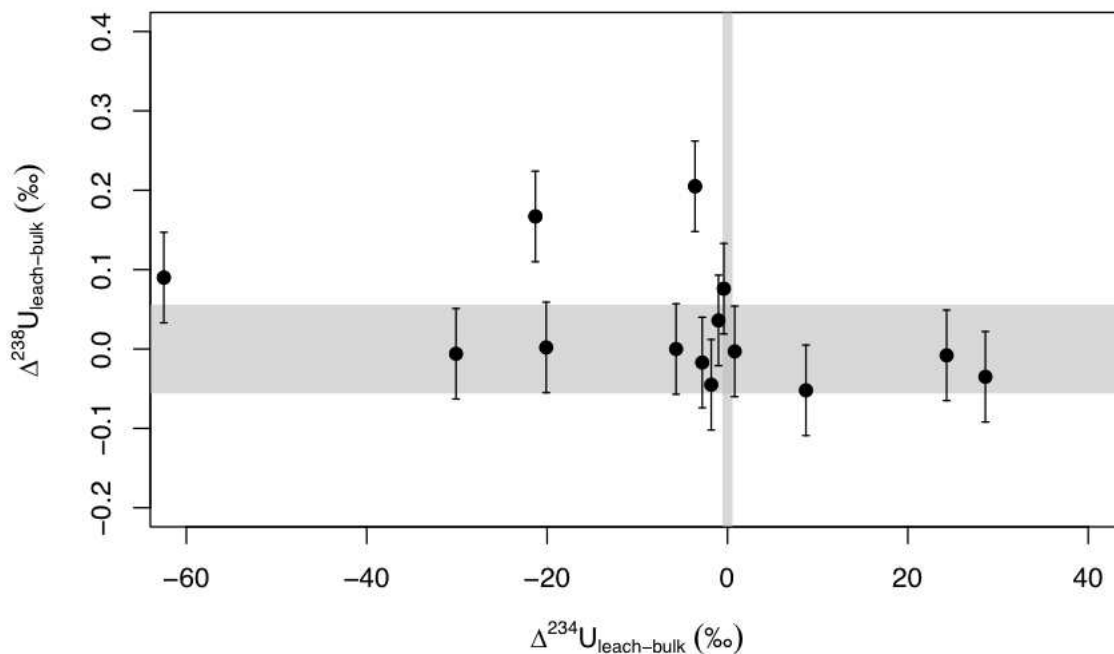
277 *Table 2: Sample description and relative difference between bulk sample and dilute sulphuric*
 278 *acid leach (24 hr) for $^{238}\text{U}/^{235}\text{U}$ and $^{234}\text{U}/^{238}\text{U}$ in permil.*

Sample ID	Mine	Granite	Country	Uranium Mineralogy	Redox	24hr leach-bulk (‰)			
						$\Delta^{238}\text{U}$	$\pm 2\text{SD}$	$\Delta^{234}\text{U}$	$\pm 2\text{SD}$
MAY_7	Botallack	Lands End	England	Bijvoetite-Y + coffinite	Reduced	0.036	0.056	-1.0	0.6
KCB5	Carbis Bay	Lands End	England	Torbernite, Zeunerite	Oxidised	-0.017	0.056	-2.8	0.6
LV2	Levant	Lands End	England	Bijvoetite-Y + coffinite		-0.008	0.056	24.3	0.6
WC1	Wheal Cock	Lands End	England	Bijvoetite-Y + coffinite, Coffinite	Reduced	-0.003	0.056	0.8	0.6
LED4	Wheal Edward	Lands End	England	Torbernite, Zeunerite	Oxidised	-0.052	0.056	8.7	0.6
OWA1	Wheal Owles	Lands End	England	Cuprosklodowskite, Uranophane	Oxidised	-0.000	0.056	-5.7	0.6
TW1	Wheal Trenwith	Lands End	England	Pb-W-Uraninite, Torbernite, Uraninite, Zeunerite	Oxidised	0.090	0.056	-62.5	0.6
WT1	Wheal Trewavas	Tregonning-Godolphin	England	Torbernite	Oxidised	0.002	0.056	-20.1	0.6
L2	Littleham Cove	Dartmoor	England	Metatyuyamunite	Reduced	0.167	0.056	-21.3	0.6
STMA1	South Terras	St Austell	England	Torbernite	Oxidised	-0.006	0.056	-30.1	0.6
SAC9	St Austell Consols	St Austell	England	Pb-W-Uraninite	Reduced	-0.035	0.056	28.6	0.6
Niger1	Niger 1	-	Niger	Pitchblende	Reduced	0.205	0.056	-3.6	0.6
S221	Site 2	Roboleiro	Portugal	Torbernite	Oxidised	0.076	0.056	-0.4	0.6
S606	Site 6	Roboleiro	Portugal	Autunite	Oxidised	-0.045	0.056	-1.8	0.6

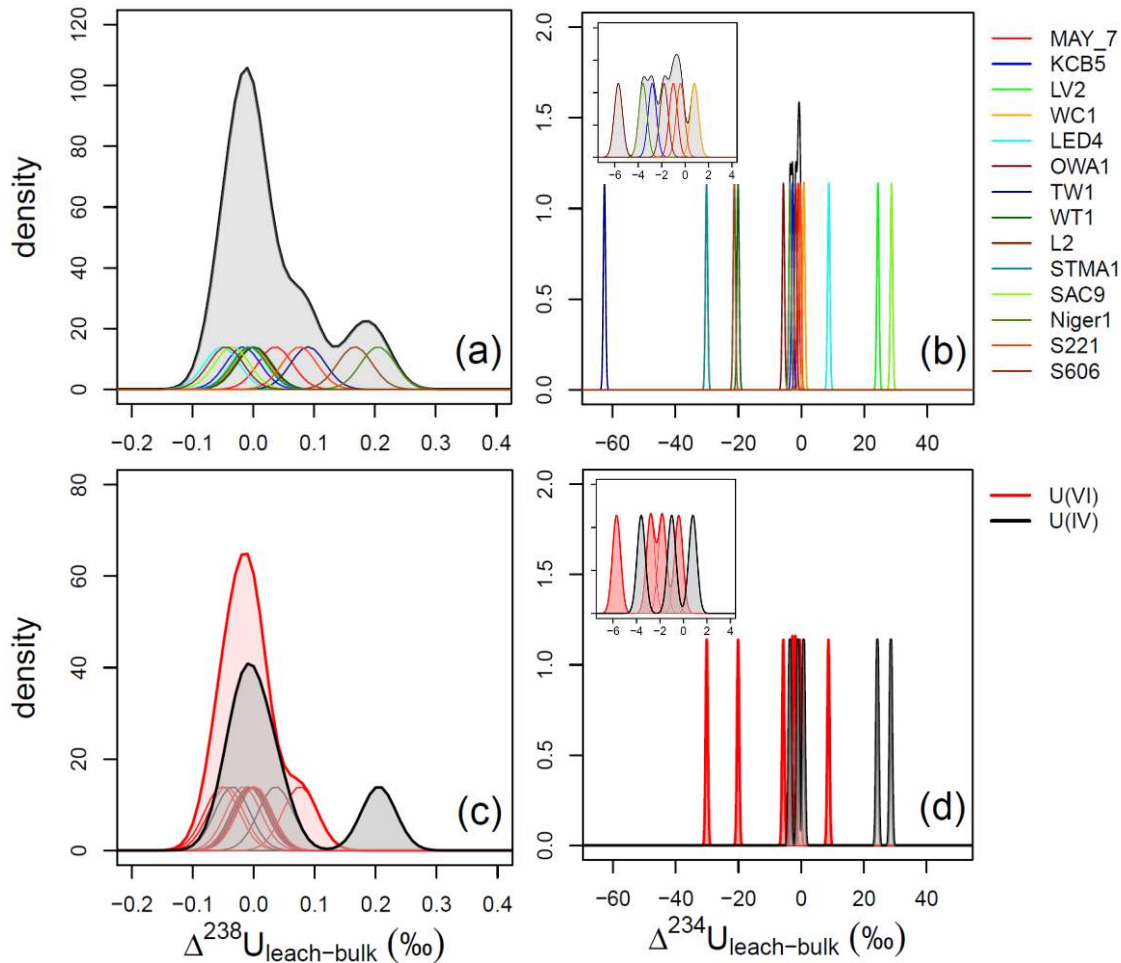
279

280 Both positive and negative values were observed for $\Delta^{238}\text{U}_{\text{leach-bulk}}$ and $\Delta^{234}\text{U}_{\text{leach-bulk}}$ (Figure 1;
 281 Figure 2). For the SW England and Portugal samples, the largest shift in $\Delta^{238}\text{U}_{\text{leach-bulk}}$ ($+0.17$
 282 ± 0.06 ‰) was sample L2 metatyuyamunite ore (Littleham Cove mine, Dartmoor, SW
 283 England), while the largest $\Delta^{234}\text{U}_{\text{leach-bulk}}$ ($+62.5 \pm 0.6$ ‰) was observed in sample TW1 (Wheal
 284 Trenwith mine, Lands End, England). Sample S221 (Roboleiro, Portugal), is the only sample
 285 that exhibited a $\Delta^{234}\text{U}_{\text{leach-bulk}}$ that did not appear to shift from 0 (-0.4 ± 0.6 ‰). Increases in
 286 $\Delta^{234}\text{U}_{\text{leach-bulk}}$ were exhibited for SAC9 and LED4 (St Austell Consols and Wheal Edward
 287 mines), while WT1, KW4, TW1, B2, STM1A and L2 (Wheal Trewavas, Kingswood mine,
 288 Wheal Trenwith, Polwheveral Creek, South Terras and Littleham Cove) show decreases. Far
 289 fewer samples display a significant shift in $\Delta^{238}\text{U}_{\text{leach-bulk}}$; all are < 0.1 ‰, apart from Niger 1

290 (+0.21 ± 0.06 ‰) and the mentioned L2 metatyuyamunite. Considering the effects of the
 291 oxidation state of U in the acid leachates (Figure 2c; 2d), it is a suggestion that $\Delta^{234}\text{U}_{\text{leach-bulk}}$ is
 292 greater for mineral phases containing reduced U(IV), while the oxidised U(VI) phases exhibit
 293 a lower $\Delta^{234}\text{U}_{\text{leach-bulk}}$.



294
 295 *Figure 1. Relative change in isotope composition ($\Delta^{234}\text{U}_{\text{leach-bulk}}$ vs $\Delta^{238}\text{U}_{\text{leach-bulk}}$) for all*
 296 *samples that were exposed to a dilute sulphuric acid leach (n=14). Shaded area represents no*
 297 *significant change in isotope ratio (where $\Delta^{234}\text{U}_{\text{leach-bulk}} = 0 \pm 0.6$ and/or $\Delta^{238}\text{U}_{\text{leach-bulk}} = 0 \pm$*
 298 *0.056).*
 299



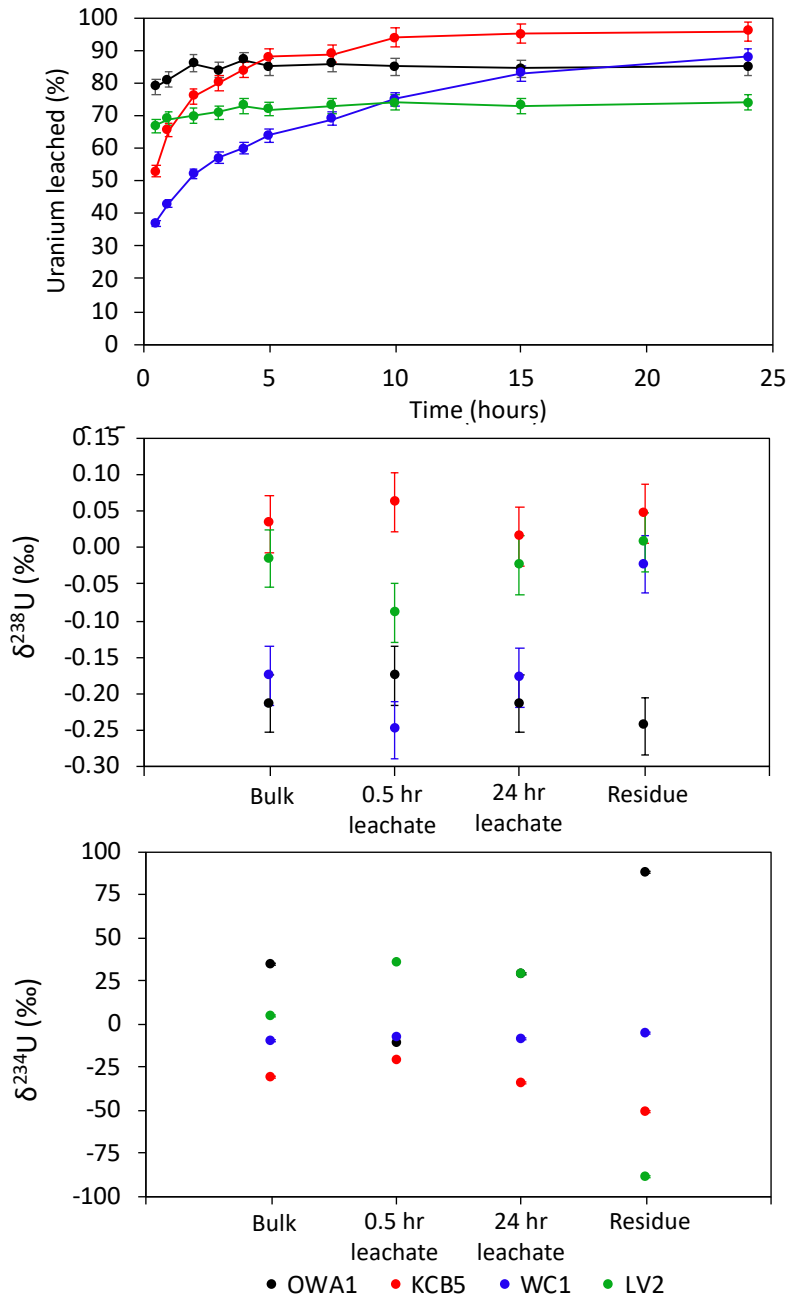
300

301 *Figure 2. Relative shift in isotope composition ($\Delta^{238}\text{U}_{\text{leach-bulk}}$ and $\Delta^{234}\text{U}_{\text{leach-bulk}}$) for a selection*
 302 *of ores after dilute sulphuric acid leach. Shaded area represents the density plots, individual*
 303 *results also shown. Data for all sites ($n=14$) in Table 2 are colour coded in (a) and (b); subsets*
 304 *of data for oxidised (red) and reduced (black) U vein samples are shown in (c) and (d) ($n=12$).*
 305

306 In addition to the 24-hr leach, aliquots of 0.5-hr leachate and residue samples were collected
 307 from two oxidised (KCB5 and LV2) and two reducing (OWA1 and WC1) U phases. Leaching
 308 profiles of the uranium ores show that > 50 % U is liberated within 2.5 hours (Figure 3). The
 309 $\delta^{238}\text{U}$ for the bulk and the 24-hr leachate are similar for each of the four veins.

310

311 For $\delta^{238}\text{U}$, the residues show similar composition to the 24-hr leachate for KCB5, OWA1 and
 312 LV2, while for WC1 the residue appears to be more enriched in ^{238}U . All four samples exhibit
 313 similar $\delta^{238}\text{U}$ as the respective bulks, for the 0.5-hr and 24-hr leachates. The $\delta^{234}\text{U}$ data show
 314 some variability for the bulk and the 24-hr leachate, OWA1, WC1 and KCB5 show similar
 315 composition, while LV2 is higher. The residue of WC1 exhibits a similar $\delta^{234}\text{U}$ composition to
 316 the 24-hr leachate, while LV2 and KCB5 are lower and OWA1 is higher.



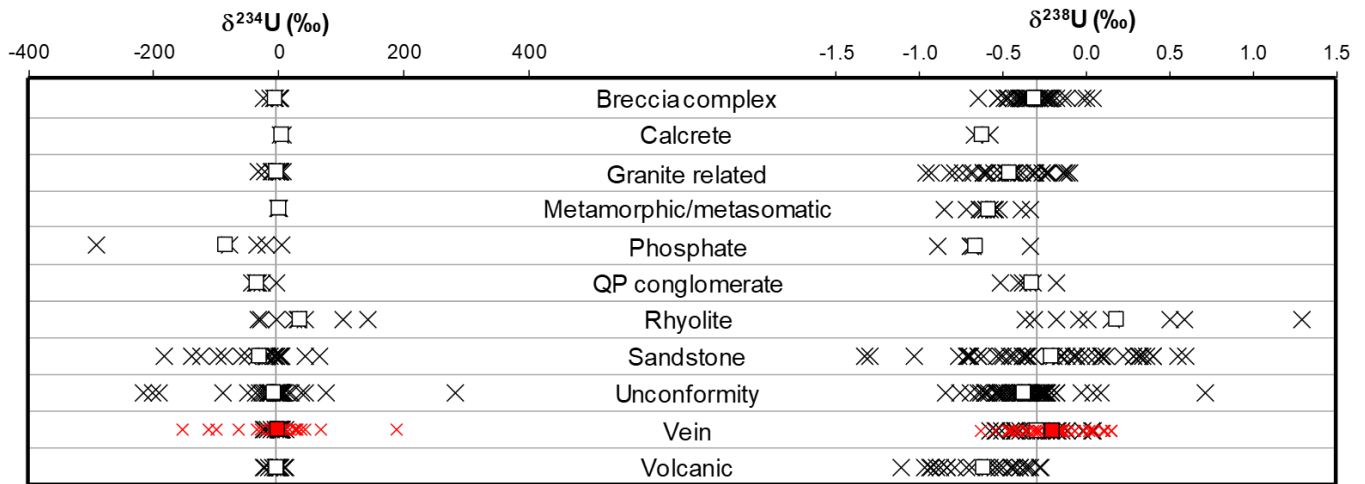
317
 318 *Figure 3. Leaching profiles of samples KCB5 (oxidised), WC1 (reduced), OWA1 (oxidised)*
 319 *and LV2 (reduced). (a) Proportion of uranium leached from ore body as a function of time.*
 320 *$\delta^{238}\text{U}$ (b) and $\delta^{234}\text{U}$ (c) for ore samples (bulk), the leachate produced after 0.5 hours of acid*
 321 *leaching, 24 hours of acid leaching and the residue remaining post-leach.*
 322

323 4 Discussion

324 325 4.1 Uranium isotope ratio variations in bulk samples

326 Since the discovery of significant natural $\delta^{238}\text{U}$ variation, several studies have analysed $\delta^{238}\text{U}$
 327 and $\delta^{234}\text{U}$ for different types of U ore deposits. Figure 4 summarises literature data for 11
 328 common U deposit types and associated U mineralisation. The data collected in this study

329 broadly fits with this literature data. The mean values for the population of data obtained in this
 330 study ($\delta^{238}\text{U} = -0.19 \pm 0.43 \text{ ‰}$, $\delta^{234}\text{U} = -6 \pm 109 \text{ ‰}$, 2σ) are similar to mean $\delta^{238}\text{U}$ and $\delta^{234}\text{U}$
 331 values for U vein type deposits in the literature, with $\delta^{234}\text{U}$ near secular equilibrium and the
 332 $\delta^{238}\text{U}$ similar to the average continental crust $\sim -0.3\text{‰}$ (Andersen et al. 2017). The range in
 333 $\delta^{238}\text{U}$ is similar, while the range in $\delta^{234}\text{U}$ measured here is larger than the compilation of the
 334 literature data for U vein-type deposits, with both higher and lower values.
 335



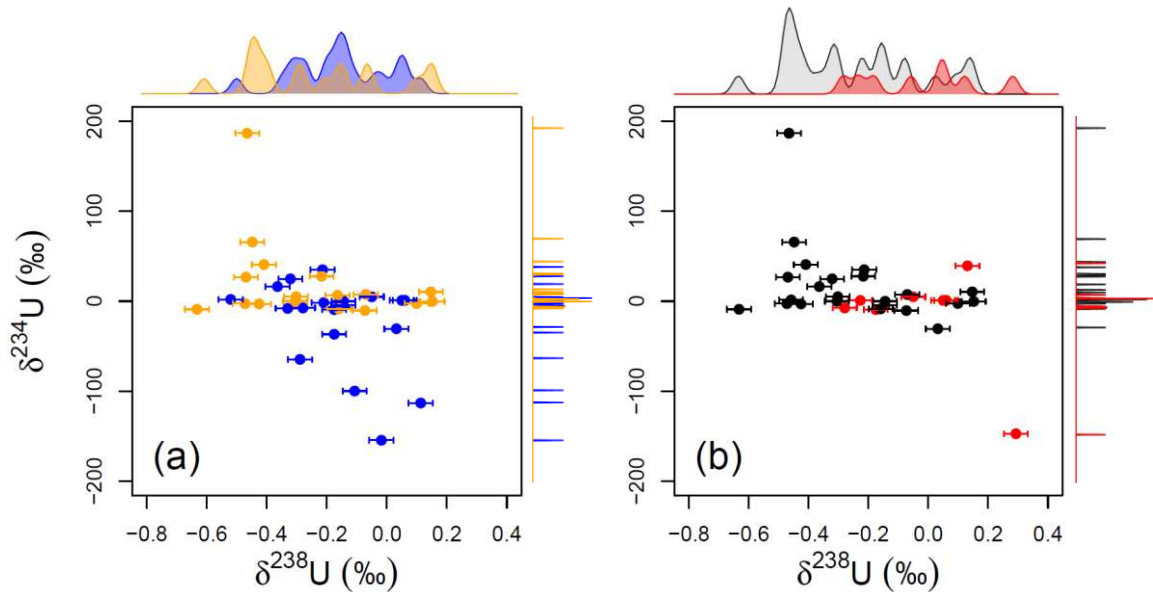
336
 337
 338 *Figure 4. Variation in $\delta^{238}\text{U}$ and $\delta^{234}\text{U}$ data for uranium ore samples of different deposit types.*
 339 *Individual data points are plotted as crosses, mean values as squares. Data from this study is*
 340 *highlighted in red. Data from Brennecka et al. (2010), Uvarova et al. (2014)*, Kirchenbaur et*
 341 *al. (2016), Chernyshev et al. (2014), Bopp et al. (2009), Golubev et al. (2013), Basu et al.*
 342 *(2015), Keegan et al. (2008), Murphy et al. (2014). * has been renormalised with a CRM129a-*
 343 *CRM112a of set -1.7 instead of -0.9 permil (see Andersen et al. 2017).*
 344
 345

346 4.2 Uranium isotope ratio variations in different locations and ore types

347 In this study, samples from SW England and Portugal were measured for $\delta^{238}\text{U}$ and $\delta^{234}\text{U}$
 348 (Figure 5a). There is a large overlap between the data sets for each of these settings: mean
 349 $\delta^{238}\text{U}$ values are $-0.16 \pm 0.33 \text{ ‰}$ (SW England), $-0.22 \pm 0.51 \text{ ‰}$ (Portugal); mean, $\delta^{234}\text{U}$ values
 350 are $-23 \pm 97 \text{ ‰}$ (SW England) and $10 \pm 110 \text{ ‰}$ (Portugal). The majority of $\delta^{234}\text{U}$ values are
 351 within $\pm 20 \text{ ‰}$ of secular equilibrium, with the samples from Portugal generally exhibiting
 352 higher $\delta^{234}\text{U}$ than those from SW England. $\delta^{238}\text{U}$ overlaps for the two regions, however there
 353 is a slight trend for samples from SW England to have higher $\delta^{238}\text{U}$ in comparison to the
 354 Portuguese samples.
 355

356 The $\delta^{238}\text{U}$ and $\delta^{234}\text{U}$ values may also be compared for uranium ore samples characterised by
 357 solely oxidised or reduced U bearing minerals (Figure 5b). Although these populations are not

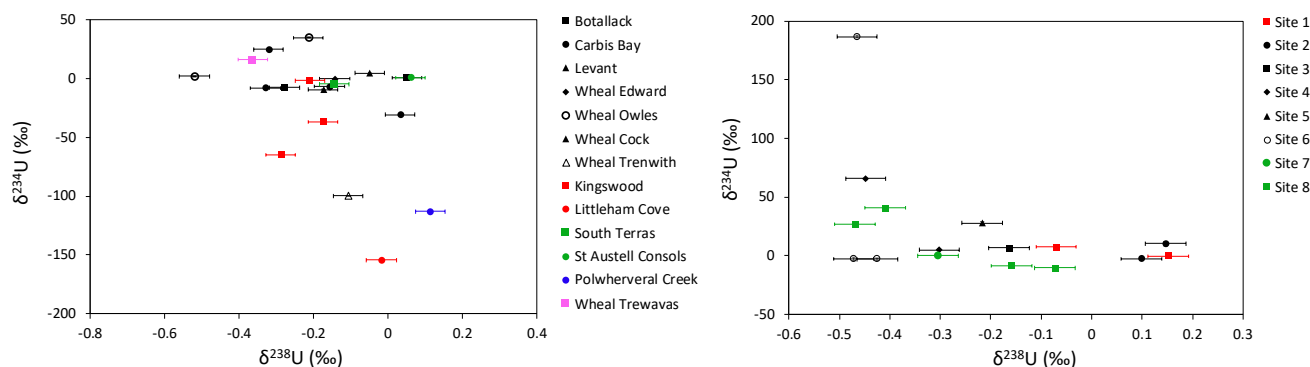
358 statistically different (as determined by a two-sample t-test), there is an apparent trend for the
 359 oxidised U minerals to exhibit a slightly lower $\delta^{238}\text{U}$ (no reduced minerals show $\delta^{238}\text{U} < -0.3$
 360 ‰, while the oxidised minerals show a larger variance (0.044 compared to 0.037). The majority
 361 of the $\delta^{234}\text{U}$ values are between 50 and -50 ‰, while the oxidised minerals exhibit a more
 362 variable $\delta^{234}\text{U}$ in comparison to the reduced minerals. This is except for one reduced U mineral
 363 sample from Niger which was highly depleted in ^{234}U ($\delta^{234}\text{U} = -147 \pm 0.4$ ‰).



364
 365 *Figure 5 (a) Variation in $\delta^{238}\text{U}$ and $\delta^{234}\text{U}$ for vein deposits of SW England (blue) and Portugal*
 366 *(orange). (b) Plot of $\delta^{238}\text{U}$ vs $\delta^{234}\text{U}$ for samples containing only oxidised (red) and only*
 367 *reduced (black) uranium minerals. Probability density plots are also shown.*
 368

369 4.3 Uranium isotope ratio variations between different mines

370 The $\delta^{238}\text{U}$ and $\delta^{234}\text{U}$ signatures for the SW England and Portugal uranium ore data sets
 371 generally overlap. Indeed, after separating the samples by region, there are no clear patterns or
 372 groupings (Figure 6). This may be ascribed to the limited number of samples. Naturally, a
 373 larger suite of samples may reveal clearer trends. When plotting the samples as individual
 374 mines it is evident that there is a particularly large range in both $\delta^{238}\text{U}$ and $\delta^{234}\text{U}$ within the
 375 Lands End granite and samples from the Roboleiro district. Except for two samples from Site
 376 6 of the Roboleiro district, samples from the same mine do not appear to have similar values.
 377



378

379 *Figure 6. Plots showing the variation in $\delta^{238}\text{U}$ vs $\delta^{234}\text{U}$ values for uranium ore (colour refers*
 380 *to associated granite and symbols individual mines) within different districts for SW England*
 381 *(a) (Black = Lands End, Red = Dartmoor, Green = St Austell, Blue = Carmenelis, Pink =*
 382 *Tregonning-Godolphin) and Portugal (b) (Red = Guarda, Black = Reboleiro, Green =*
 383 *Urgeiriça).*

384

385 4.4 Uranium isotope ratio variations within the same mine and vein

386 Variable $\delta^{238}\text{U}$ and $\delta^{234}\text{U}$ values are obtained for samples collected from along the same
 387 mineral vein at Kingswood and Carbis Bay (Figure 7). For the samples taken from three
 388 different positions along the Kingswood mineral vein, the most enriched sample in ^{238}U was
 389 KW10 ($\delta^{238}\text{U} = -0.18 \pm 0.04 \text{ ‰}$), while the most depleted was KW12 ($\delta^{238}\text{U} = -0.29 \pm 0.04$
 390 ‰). Based on single factor ANOVA, there is a significant statistical difference between these
 391 samples. Similarly, the mean $\delta^{234}\text{U}$ values are statistically different (single factor ANOVA),
 392 and decrease along the mineral vein. The most enriched sample in ^{234}U along the Kingswood
 393 vein was KW4 ($\delta^{234}\text{U} = -1.5 \pm 0.4 \text{ ‰}$) and the most depleted was KW12 ($\delta^{234}\text{U} = -64.7 \pm 0.4$
 394 ‰).

395 Two samples were collected from the start and end of two veins (KCB and CBJ) within 10 m
 396 of one another from a mine at Carbis Bay (Figure 7c; 7d). Although uncertainties overlap at
 397 the 95 % confidence level, two sample t-tests (significance level, α , of 0.05) show that there is
 398 a statistical difference in the mean $\delta^{238}\text{U}$ values for the two samples from vein CBJ (CBJ1 =
 399 $-0.35 \pm 0.04 \text{ ‰}$, CBJ6 = $-0.32 \pm 0.04 \text{ ‰}$). Additionally, the $\delta^{238}\text{U}$ for the samples from vein
 400 KCB show greater variability (KCB1 = $-0.16 \pm 0.04 \text{ ‰}$, KCB5 = $+0.030 \pm 0.04 \text{ ‰}$) (Figure
 401 7c). The $\delta^{234}\text{U}$ for the two samples collected from each of the two veins at Carbis Bay are
 402 statistically different (CBJ1 = $-16.0 \pm 0.4 \text{ ‰}$, CBJ6 = $24.9 \pm 0.4 \text{ ‰}$; KCB1 = $-6.6 \pm 0.4 \text{ ‰}$,
 403 KCB5 = $-30.6 \pm 0.4 \text{ ‰}$). In summary, these measurements show evidence of a heterogeneous
 404 U isotopic composition (for both $\delta^{234}\text{U}$ and $\delta^{238}\text{U}$) for samples collected from within the same
 405 mine and from the same vein.

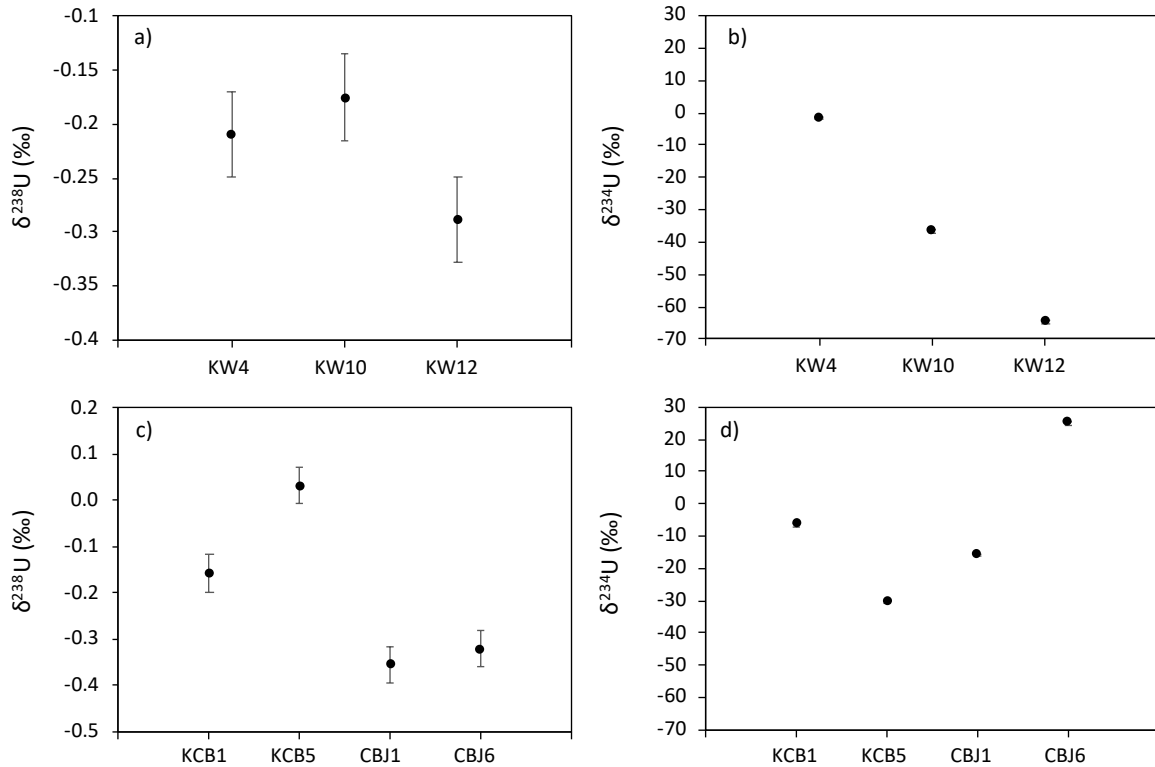


Figure 7. Variation in $\delta^{238}\text{U}$ vs $\delta^{234}\text{U}$ within the Kingswood mineral vein (a, b) and the two Carbis Bay mineral veins (c, d). Typical uncertainties for $\delta^{234}\text{U}$ are smaller than the marker.

4.5 Processes responsible for the uranium isotope ratio variations

Here we discuss the specific U isotope signatures in the samples analysed, focusing firstly on mechanisms that influence $\delta^{234}\text{U}$ and then $\delta^{238}\text{U}$.

4.5.1 $\delta^{234}\text{U}$ signatures in the vein ore minerals

One key observation is that most of the bulk samples analysed are in a state of U-series disequilibrium ($\delta^{234}\text{U}$ deviating from 0). The samples with oxidised U minerals are determined to be more variable and exhibit higher $\delta^{234}\text{U}$, whereas samples with reduced U minerals show less variability and more samples with $\delta^{234}\text{U} < 0$ (Figure 5b). Disequilibrium in $^{234}\text{U}/^{238}\text{U}$ has been associated with localized crystal damage induced by α -recoil processes and can be achieved in several ways in uranium-rich ore samples, both from physical redistribution at steady-state and from non-steady state chemical weathering processes. In a heterogeneous sample containing phases with different U concentrations, α -recoil processes may re-distribute ^{234}U across grain boundaries from high to low U phases, leading to $\delta^{234}\text{U}$ below and above 0 in each medium, respectively. This process may occur at steady-state, thus being independent

426 of the decay rates and time. In this scenario, the high U-containing mineral phases, as sampled
427 in this study would be expected to exhibit $\delta^{234}\text{U}$ values < 0 . This could explain some of the
428 observed data, but not the samples with $\delta^{234}\text{U}$ above secular equilibrium. Thus, the data
429 suggests that the observed disequilibrium is likely associated with more recent weathering-
430 driven U mobility. Preferential mobility of ^{234}U during oxidative weathering and leaching,
431 generally leads to a residue below secular equilibrium and excess ^{234}U in a dissolved form. In
432 addition, adsorption of ^{234}U to mineral phases (e.g. via the short-lived ^{234}Th daughter), provides
433 one mechanism for samples to obtain $\delta^{234}\text{U} > 0$. Reprecipitation of U minerals from dissolved
434 U-rich geofluids, with excess ^{234}U from U vein leaching, provides an alternative mechanism.
435 These observations suggest that the variable $\delta^{234}\text{U}$ in the U ores is likely linked to recent (< 2.5
436 Ma) processes of U mobility associated with the redistribution of U daughter isotopes from
437 within the ore systems. This trend may explain the characteristic difference between the
438 Portuguese and English U vein samples. All Portuguese samples are secondary minerals.
439 Therefore, it is possible that the excess ^{234}U in many of these samples is a result of secondary
440 mineralisation of U leached from a primary ore with a high $\delta^{234}\text{U}$. Furthermore, relatively low
441 rainfall, as occurring in the regions of the Portuguese samples, promotes high $\delta^{234}\text{U}$ in the
442 dissolved U fluids via increased residence times and water-rock interaction (Robinson et al.
443 2004). In contrast, the SW England samples may represent older primary uranium phases where
444 ^{234}U has been preferentially leached and therefore generally lower $\delta^{234}\text{U}$. Indeed, this
445 suggestion is strengthened by the observation that these SW England samples were sourced
446 from tailings piles and old mine adits (> 100 years old) that have been continuously leached by
447 meteoric waters.

448

449 $\Delta^{234}\text{U}_{\text{leach-bulk}}$ also varies considerably between the majority of leachates relative to the bulk
450 (Figure 1; Figure 2; Figure 3). Some of the reduced U minerals show an excess of ^{234}U in the
451 leachates, which could be attributed to preferential release of ^{234}U from damaged crystal lattice
452 sites. The oxidised U ores, however, generally show lower ^{234}U in the leachates than the bulk,
453 which suggest limited preferential release of ^{234}U and incongruent dissolution of areas with
454 lower $\delta^{234}\text{U}$ (e.g. near grain boundaries). Taken together it suggests that the reduced U minerals
455 are generally of older origin and susceptible to preferential release of ^{234}U , while the majority
456 of the oxidised U minerals are likely precipitated from U-rich fluids as secondary phases
457 produced from weathering processes via U vein dissolution within the vein system.

458

459 4.5.2 $\delta^{238}\text{U}$ signatures in the vein ore minerals

460 The U ores samples show a large variability of $\sim 1\text{‰}$ in $\delta^{238}\text{U}$ (Figure 4). The reduced U
461 mineral samples range from the average crustal value (-0.3‰) and to higher values ($+0.3\text{‰}$),
462 while the oxidised U minerals are similarly high, but extend to lower compositions (-0.6‰).
463 The overall lower $\delta^{238}\text{U}$ for the oxidised U minerals relative to the reduced U mineral samples
464 agrees well with the expected U isotope fractionation during U redox transformations,
465 favouring the ^{238}U in the reduced U^{4+} phases (Bigeleisen, 1996). The cause of the similar $\delta^{238}\text{U}$
466 observed for oxidised and reduced U minerals is analogous to an interpretation applied to $\delta^{234}\text{U}$:
467 the oxidised U minerals are secondary phases derived from the oxidation and dissolution of
468 reduced U minerals in a different part of the ore system. Experimental studies have shown only
469 minor U isotope fractionation ($< 0.2\text{‰}$) for the oxidation of uraninite minerals (Wang et al.
470 2015) which fits with the similar, but slightly lower $\delta^{238}\text{U}$ for the oxidised U minerals. The
471 minor variability in $\delta^{238}\text{U}$ for some leachates relative to the bulk (Figure 1; Figure 2; Figure 3),
472 may indicate isotope fractionation or artifacts from re-adsorption processes during this leaching
473 (Wang et al. 2015) or the dissolution of discrete areas or phases with different $\delta^{238}\text{U}$
474 (Chernyshev et al., 2014). While the both the oxidised and reduced U mineral samples show
475 an increase in $\Delta^{238}\text{U}_{\text{leach-bulk}}$ (Figure 2), the progressive leaching studies (Figure 3) show no
476 systematic change in $\Delta^{238}\text{U}_{\text{leach-bulk}}$ for any of the samples. Thus, it is likely that the variable
477 $\Delta^{238}\text{U}_{\text{leach-bulk}}$ are from a combination of the two above processes (isotope fractionation during
478 leaching/absorption and pre-existing sample heterogeneity).

479

480 4.6 Implications for nuclear forensics

481 Isotopic measurements of uranium materials have been successfully deployed in nuclear
482 forensics investigations as comparative signatures to determine the provenance UOCs out of
483 regulatory control. The methodology compares material characteristics of a seized sample of
484 unknown origin to a database of previously characterised samples of known origin. This allows
485 direct attribution or in the least, ruling out specific material sources. In addition to utilising the
486 U isotopic composition as a forensic indicator, other distinguishing material characteristics
487 may include, the major molecular species, isotopic composition of S, O, Sr, Nd, Mo and Pb,
488 elemental and anionic impurities, rare earth element pattern and concentrations (Han et al.
489 2013; Keegan et al. 2014; Rolison et al. 2019; Migeon et al. 2020). This equates to
490 approximately 50 discrete signature variables. A range of statistical tools may subsequently be
491 used to relate the unknown material to a characterised database sample (Keegan et al. 2012;

492 Corcoran et al. 2019). Although $\delta^{234}\text{U}$ and $\delta^{238}\text{U}$ may only represent two of these 50 potential
493 variables, they have previously been recognised as key comparative discriminators (Keegan et
494 al. 2016). It is therefore important for the nuclear forensics practitioner to acknowledge
495 potential perturbation of these signatures based on observations made in this study: localised
496 isotopic heterogeneity and changes in the U isotope composition caused by a weak sulphuric
497 acid leach.

498
499 If the uranium isotope ratios remained unchanged during processing of ore to UOC, the data
500 suggest that taken broadly, the $\delta^{238}\text{U}$ reflect the ore's original depositional setting (e.g.
501 depositional redox conditions) allowing individual deposit types to be separated. The $\delta^{234}\text{U}$ is
502 regarded as being site specific and will depend on several conditions e.g. water-rock interaction
503 history within the last 1-2 million years will be linked to the age, permeability and structure of
504 the deposit. Therefore, $\delta^{238}\text{U}$ and $\delta^{234}\text{U}$ may be deployed as separate nuclear forensic
505 signatures; $\delta^{238}\text{U}$ predictively, whereas $\delta^{234}\text{U}$ is more site specific (Brennecka et al., 2010).

506
507 The experiments here demonstrate uranium isotope heterogeneity for samples collected from
508 the same mine, albeit on an extremely small sample scale (~ 1 g) relative to industrial scale ore
509 extraction. Based on the relatively large variability in these samples and within single mines,
510 isotopic heterogeneity may be expected regardless of the amount of ore extracted. There is no
511 evidence to suggest that sampling a sufficiently large quantity of ore may yield a non-variable
512 uranium isotope ratio that is representative of the respective mine. Therefore, if different
513 batches of UOC have been produced by a processing facility using uranium ore from different
514 extraction events at the same mine, it is not necessarily valid to assign a fixed value for the
515 uranium isotopic composition of a UOC.

516
517 Following dilute sulphuric acid treatment to simulate industrial ore processing, significant
518 differences between the $\delta^{238}\text{U}$ values of bulk solid (ore) and leachate (processed
519 material) were observed for a limited number of samples in this study, and for $\delta^{234}\text{U}$ this was
520 the case for nearly all samples (Figure 1). This contrasts with results of a study comparing
521 two uraninite specimens (feed material) to four samples of product UOC material from the
522 Willow Creek Project (South Powder River Uranium district, Wyoming) for which $^{238}\text{U}/^{235}\text{U}$
523 and $^{234}\text{U}/^{238}\text{U}$ remained broadly consistent (Spano et al. 2017). Based on these findings, the
524 study concluded that any changes to the U isotopic signature caused during early ore

525 processing were insignificant. It is possible that different conclusions have been reached
526 because of the limited number of samples and single location studied in Spano et al. 2017.

527

528 In the context of nuclear forensics and comparing the $\delta^{234}\text{U}$ and $\delta^{238}\text{U}$ of a UOC of known
529 provenance to an unknown seized sample, there is potential for UOC processing to modify the
530 uranium isotope compositions and consequently mislead an investigation. For example, where
531 a UOC of known provenance and an unknown seized UOC are sourced from the same mine
532 but processed at different points in time (i.e. as different batches), inconsistent isotopic
533 compositions caused by batch to batch variance may lead an analyst to incorrectly conclude
534 the two samples are different. Although the reproducibility of these observed changes in
535 isotopic composition have not been studied here, when considering the variability of $\delta^{234}\text{U}$ and
536 $\delta^{238}\text{U}$ in nature, it is conceivable that a dilute sulphuric acid leach may yield a variable U
537 isotope signature. We recommend future studies in this area to evaluate the reproducibility of
538 U isotope changes caused during these chemical processes that are typical of the nuclear fuel
539 cycle.

540

541 Localised isotopic heterogeneity and changes to the U isotope signature caused by a weak
542 sulphuric acid leach have the potential to mislead a nuclear forensics investigation where $\delta^{234}\text{U}$
543 and $\delta^{238}\text{U}$ are relied upon. The circumstances discussed above highlight the requirement for a
544 subject matter expert (SME) to review these signature data prior to applying the subsequent
545 statistical tools associated with the comparative signature approach. We recommend the
546 respective SME is aware of the potential for perturbation of $\delta^{234}\text{U}$ and $\delta^{238}\text{U}$ as highlighted in
547 this paper. While there is some potential for these signatures to misinform, it is important to
548 recognise that the analytical techniques used in this study quote more precise values ($\pm 0.04\text{‰}$
549 for $\delta^{238}\text{U}$ and $\pm 0.4 \text{‰}$ for $\delta^{234}\text{U}$) relative to those given in the nuclear forensics investigation
550 reported in Keegan et al. (2016) (relative uncertainty $k=3$, $^{235}\text{U}/^{238}\text{U} = 0.2 \text{‰}$, $^{234}\text{U}/^{238}\text{U} = 0.6$
551 ‰). At these lower precisions it is not possible to discriminate between the differences in
552 isotopic composition as discussed in this paper. While this may trivialise the issue of changes
553 to the U isotopic composition during processing, less precise data inevitably reduce the
554 discriminatory power of these signatures.

555

556 5 Conclusions

557

558 In this study, $\delta^{238}\text{U}$ and $\delta^{234}\text{U}$ have been determined for vein type uranium ore deposits
559 collected mainly from mines in central Portugal and SW England. The data presented are in
560 agreement with mean $\delta^{238}\text{U}$ and $\delta^{234}\text{U}$ values for other vein type uranium deposits reported
561 elsewhere in the literature. Notably, the range in $\delta^{234}\text{U}$ measured here is significantly larger
562 than current available literature data for U vein type deposits, with both negative and positive
563 values with respect to secular equilibrium.

564
565 There is overlap between $\delta^{238}\text{U}$ and $\delta^{234}\text{U}$ values obtained for samples from SW England and
566 Portugal. However, there is a tendency for the Portuguese $\delta^{234}\text{U}$ to be higher relative to the
567 English samples and vice versa for $\delta^{238}\text{U}$. It was not possible to use these signatures to
568 distinguish between different regions of the same country or different mines of the same
569 country. When comparing reduced U versus oxidised U mineral phases, we observe a
570 distribution with lower average $\delta^{238}\text{U}$ values for oxidised U samples, which follows the nuclear
571 field shift theory for U isotope fractionation observed elsewhere. Although it is expected that
572 U isotopic heterogeneity within the sample will also play a role in this observation. The
573 majority of the $\delta^{234}\text{U}$ values are close to secular equilibrium, but some of the U^{6+} (uranyl)
574 minerals exhibit considerably more variable $\delta^{234}\text{U}$, suggesting within mine mobility of U
575 within the last two million years.

576
577 Variable $\delta^{238}\text{U}$ and $\delta^{234}\text{U}$ are observed for samples collected from within the same mine and
578 vein at the Carbis Bay and Kingswood mines. Leaching several of these samples in dilute
579 sulphuric acid for 24 hours caused both $^{235}\text{U}/^{238}\text{U}$ and $^{234}\text{U}/^{238}\text{U}$ to change unpredictably. The
580 dissimilar patterns of $\delta^{238}\text{U}$ and $\delta^{234}\text{U}$ indicate these two signatures are decoupled and rely on
581 different mechanisms. These findings suggest UOCs produced from ore extracted from the
582 same mine, via the same procedures, can yield variable $\delta^{238}\text{U}$ and $\delta^{234}\text{U}$.

583

584 Acknowledgements

585
586 The authors wish to extend thanks to the Cabot Institute, University of Bristol, for supporting
587 this work and AWE plc for funding [contract reference: 30218761]. Additional thanks to Tim
588 Elliott and Christopher Coath, Bristol Isotope Group, University of Bristol. The authors also
589 wish to acknowledge Laboratório de Protecção e Segurança Radiológica at Unidade de
590 Protecção e Segurança Radiológica for their assistance during fieldwork and sample collection.

591

592 References

593

594 Abe, M., Suzuki, T., Fujii, Y., Hada, M., Hirao, K., 2008. An ab initio molecular orbital study
595 of the nuclear volume effects in uranium isotope fractions. *J. Chem. Phys.* 129, 16.

596 <https://doi: 10.1063/1.2992616>

597 Andersen, M.B., Elliott, T., Freymuth, H., Sims, K.W.W., Niu, Y., Kelley, K. A., 2015. The
598 terrestrial uranium isotope cycle. *Nature* 517, 356–359.

599 <https://doi.org/10.1038/nature14062>

600 Andersen, M.B., Romaniello, S., Vance, D., Little, S.H., Herdman, R., Lyons, T. W., 2014. A
601 modern framework for the interpretation of $^{238}\text{U}/^{235}\text{U}$ in studies of ancient ocean redox.

602 *Earth Planet. Sci. Lett.* 400, 184 – 194. <https://doi.org/10.1016/j.epsl.2014.05.051>

603 Andersen, M., Stirling, C., Weyer, S., 2017. Uranium isotope fractionation. *Reviews in*
604 *Mineralogy and Geochemistry* 82(1), 799–850. <https://doi.org/10.2138/rmg.2017.82.19>

605 Basu, A., Brown, S.T., Christensen, J.N., DePaolo, D.J., Reimus, P.W., Heikoop, J.M.,
606 Woldegabriel, G., Simmons, A.M., House, B.M., Hartmann, M., Maher, K., 2015.

607 Isotopic and geochemical tracers for U(VI) reduction and U mobility at an in situ
608 recovery U mine. *Environ. Sci. Technol.* 49, 5939–5947.

609 <https://doi.org/10.1021/acs.est.5b00701>

610 Bigeleisen, J., Nuclear size and shape effects in chemical reactions. *Isotope chemistry of the*
611 *heavy elements.* *J. Am. Chem. Soc.* 118, 3676–3680. <https://doi.org/10.1021/ja954076k>

612 Bodu R., Bouzigues H., Morin N., Pfiffelmann J.P., 1972. Sur l'existence d'anomalies

613 isotopiques rencontrées dans l'uranium du Gabon. *C. R. Acad. Sci. Paris.* 275, 1731–
614 1734.

615 Bopp, C.J., Lundstrom, C.C., Johnson, T.M., Glessner, J.J.G., 2009. Variations in $^{238}\text{U}/^{235}\text{U}$
616 in uranium ore deposits: Isotopic signatures of the U reduction process? *Geology* 37,

617 611–614. <https://doi.org/10.1130/G25550A.1>

618 Brennecka, G. a., Borg, L.E., Hutcheon, I.D., Sharp, M. a. ore, Anbar, A.D., 2010. Natural
619 variations in uranium isotope ratios of uranium concentrates: Understanding the
620 $^{238}\text{U}/^{235}\text{U}$ fractionation mechanism. *Earth Planet. Sci. Lett.* 291, 228–233.

621 <https://doi.org/10.1016/j.epsl.2010.01.023>

622 Cameron, J., 1982a. *Geomorphology and the Uranium Vein Deposits of the Beira Region of*
623 *Portugal*, IAEA. IAEA, Vienna, Austria.

624 Cameron, J., 1982b. *Mineralogical Aspects and Origin of the Uranium in the Vein Deposits*
625 *of Portugal*, IAEA. IAEA, Vienna, Austria.

626 Cheng, H., Edwards, R.L., Sehe, C.C., Polyak, V.J., Asmerom, Y., Woodhead, J., Hellstrom,
627 J., Wang, Y., Kong, X., Spoetl, C., Wang, X., Alexander Jr., E. C., 2013. Improvements

628 in ^{230}Th dating, ^{230}Th and ^{234}U half-life values, and U-Th isotopic measurements by
629 multi-collector inductively coupled plasma mass spectrometry. *Earth Planet. Sci. Lett.*

630 371–372, 82–91. <https://doi.org/10.1016/j.epsl.2013.04.006>

631 Chernyshev, I. V., Golubev, V.N., Chugaev, a. V., Baranova, a. N., 2014. $^{238}\text{U}/^{235}\text{U}$ isotope
632 ratio variations in minerals from hydrothermal uranium deposits. *Geochemistry Int.* 52,

633 1013–1029. <https://doi.org/10.1134/S0016702914120027>

634 Corcoran, L., Simonetti, A., Spano, T. L., Lewis, S. R., Dorais, C., Simonetti, S., Burns, P.
635 C., 2019. Multivariate analysis based on geochemical, isotopic, and mineralogical

636 compositions of uranium-rich samples. *Minerals*, 9(9), 537.

637 <https://doi.org/10.3390/min9090537>

638 Cowan, G., Adler, H.H., 1976. The variability of the natural abundance of ^{235}U . *Geochim.*
639 *Cosmochim. Acta* 40, 1487–1490. [https://doi.org/10.1016/0016-7037\(76\)90087-9](https://doi.org/10.1016/0016-7037(76)90087-9)

640 Golubev, V.N., Chernyshev, I. V, Chugaev, A. V, Eremina, A. V, Baranova, A.N.,

641 Krupskaya, V. V, 2013. U – Pb Systems and U Isotopic Composition of the Sandstone

642 Hosted Paleovalley Dybryn Uranium Deposit , Vitim Uranium District, Russia 55, 399–
643 410. <https://doi.org/10.1134/S1075701513060044>

644 Hiess, J., Condon, D. J., McLean, N. & Noble, S. R., 2012. $^{238}\text{U}/^{235}\text{U}$ systematics in terrestrial
645 uranium-bearing minerals. *Science* 335, 1610–1614.
646 <https://doi.org/10.1126/science.1215507>

647 IAEA, 2006. Nuclear Forensics Support Reference Manual.

648 IAEA, 1993. 359 Uranium Extraction Technology.

649 Ivanovitch, M., 1992. Uranium-series disequilibrium: applications to earth, marine, and
650 environmental sciences. 2. ed. 910 p; Clarendon Press; Oxford, UK.

651 Keatley, AC, Scott, TB, Davis, S & Jones, CP, 2015, ‘An investigation into heterogeneity in
652 a single vein-type uranium ore deposit: Implications for nuclear forensics’. *Journal of*
653 *Environmental Radioactivity*, vol 150., pp. 75-85.
654 <https://doi.org/10.1016/j.jenvrad.2015.06.016>

655 Keatley, A.C., 2016. An investigation into the heterogeneity of vein type uranium ore
656 deposits: Implications for nuclear forensic analysis. University of Bristol.

657 Keatley, AC, Martin, PG, Hallam, KR, Payton, OD, Awbery, R, Carvalho, F, Oliveira, JM,
658 Silva, L, Malta, M & Scott, TB, 2018, ‘Source identification of uranium-containing
659 materials at mine legacy sites in Portugal’. *Journal of Environmental Radioactivity*, vol
660 183., pp. 102-111. 10.1016/j.jenvrad.2017.12.009

661 Keegan, E., Kristo, M.J., Colella, M., Robel, M., Williams, R., Lindvall, R., Eppich, G.,
662 Roberts, S., Borg, L., Gaffney, A., Plaue, J., Wong, H., Davis, J., Loi, E., Reinhard, M.,
663 Hutcheon, I., 2014. Nuclear forensic analysis of an unknown uranium ore concentrate
664 sample seized in a criminal investigation in Australia. *Forensic Sci. Int.* 240, 111–121.
665 <https://doi.org/10.1016/j.forsciint.2014.04.004>

666 Keegan, E., Richter, S., Kelly, I., Wong, H., Gadd, P., Kuehn, H., Alonso-Munoz, A., 2008.
667 The provenance of Australian uranium ore concentrates by elemental and isotopic
668 analysis. *Appl. Geochemistry* 23, 765–777.
669 <https://doi.org/10.1016/j.apgeochem.2007.12.004>

670 Keegan, E., Wallenius, M., Mayer, K., Varga, Z., Rasmussen, G., 2012. Attribution of
671 uranium ore concentrates using elemental and anionic data. *Appl. Geochemistry* 27, 8,
672 1600-1609. <https://doi.org/10.1016/j.apgeochem.2012.05.009>

673 Kigoshi, K., 1971. Uranium-234/Uranium-238. *Science* 80, 173, 47–48.

674 Kirchenbaur, M., Maas, R., Ehrig, K., Kamenetsky, V.S., Strub, E., Ballhaus, C., Münker, C.,
675 2016. Uranium and Sm isotope studies of the supergiant Olympic Dam Cu-Au-U-Ag
676 deposit, South Australia. *Geochim. Cosmochim. Acta* 180, 15–32.
677 <https://doi.org/10.1016/j.gca.2016.01.035>

678 Kristo, M.J., Gaffney, A.M., Marks, N., Knight, K., Cassata, W.S., Hutcheon, I.D., 2016.
679 Nuclear Forensic Science: Analysis of Nuclear Material Out of Regulatory Control.
680 *Annu. Rev. Earth Planet. Sci.* 2016, 44, 555-579. <https://doi.org/10.1146/annurev-earth-060115-012309>

681

682 Kristo, M.J., Tumey, S.J., 2013. The state of nuclear forensics. *Nucl. Instruments Methods*
683 *Phys. Res. Sect. B Beam Interact. with Mater. Atoms* 294, 656–661.
684 <https://doi.org/10.1016/j.nimb.2012.07.047>

685 Lewis, S. R., Simonetti, A., Corcoran, L., Simonetti, S. S., Dorais, C., Burns, P. C., 2020.
686 The role of continental crust in the formation of uraninite-based ore deposits. *Minerals*
687 10, 136. <https://doi.org/10.3390/min10020136>

688 Migeon, V., Fitoussi, C., Pili, E., Bourdon, B., 2020. Molybdenum isotopic fractionation in
689 uranium oxides and during key processes of the nuclear fuel cycle: Towards a new
690 nuclear forensic tool. *Geochim. Cosmochim. Acta.* 279, 238-257.
691 <https://doi.org/10.1016/j.gca.2020.03.046>

692 Murphy, M.J., Stirling, C.H., Kaltenbach, A., Turner, S.P., Schaefer, B.F., 2014.
693 Fractionation of $^{238}\text{U}/^{235}\text{U}$ by reduction during low temperature uranium mineralisation
694 processes. *Earth Planet. Sci. Lett.* 388, 306–317.
695 <https://doi.org/10.1016/j.epsl.2013.11.034>

696 Robinson, L.F., Henderson, G.M., Hall, L. and Matthews, I., 2004. Climatic control of
697 riverine and seawater uranium-isotope ratios. *Science*, 305 (5685), 851-854.
698 <https://doi.org/10.1126/science.1099673>.

699 Rolison, J. M., Druce, M., Shollenberger, Q. R., Kayzar-Boggs, T. M., Lindvall, R. E.,
700 Wimpenny, J., 2019. Molybdenum isotope compositions of uranium ore concentrates by
701 double spike MC-ICP-MS. *Appl. Geochemistry*, 103, 97-105.
702 <https://doi.org/10.1016/j.apgeochem.2019.03.001>

703 Russell, W.A., Papanastassiou, D.A., Tombrello, T.A., 1978. Ca isotope fractionation on the
704 earth and other solar system materials. *Geochim. Cosmochim. Acta* 42, 1075-1090.
705 [https://doi.org/10.1016/0016-7037\(78\)90105-9](https://doi.org/10.1016/0016-7037(78)90105-9)

706 Sheng, Z.Z., Kuroda, P.K., 1986a. Isotopic Fractionation of Uranium: Extremely High
707 Enrichments of ^{234}U in the Acid-Residues of a Colorado Carnotite. *Radiochim. Acta*
708 39, 131–138. <https://doi.org/10.1524/ract.1986.39.3.131>

709 Sheng, Z.Z., Kuroda, P.K., 1986b. Further Studies on the Separation Acid Resdues with
710 Extremely High $^{234}\text{U}/^{238}\text{U}$ Ratios from a Colorado Carnotite. *Radiochim. Acta* 40, 95–
711 102.

712 Spano, T. L., Simonetti, A., Balboni, E., Dorais C., Burns P. C., 2017. Trace element and U
713 isotope analysis of uraninite and orc concentrate: Applications for nuclear forensics
714 investigations. *Appl. Geochemistry*. 84, 277-285.
715 <http://dx.doi.org/10.1016/j.apgeochem.2017.07.003>

716 Stirling, C.H., Andersen, M.B., Potter, E.K., Halliday, A.N., 2007. Low-temperature isotopic
717 fractionation of uranium. *Earth Planet. Sci. Lett.* 264, 208–225.
718 <https://doi.org/10.1016/j.epsl.2007.09.019>

719 Sun-Ho H., Varga, Z., Kajko, J., Wallenius, M., Song, K., Mayer, K., 2013. Measurement of
720 the sulphur isotope ratio ($^{34}\text{S}/^{32}\text{S}$) in uranium ore concentrates (yellow cakes) origin
721 assessment. *J. Anal. At. Spectrom.*, 28, 1919-1925.
722 <https://doi.org/10.1039/C3JA50231G>

723 Uvarova, Y. a., Kyser, T.K., Geagea, M.L., Chipley, D., 2014. Variations in the uranium
724 isotopic compositions of uranium ores from different types of uranium deposits.
725 *Geochim. Cosmochim. Acta* 146, 1–17. <https://doi.org/10.1016/j.gca.2014.09.034>

726 Wang, X., Johnson, T.M., Lundstrom, C.C., 2015. Isotope fractionation during oxidation of
727 tetravalent uranium by dissolved oxygen. *Geochim. Cosmochim. Acta* 150, 160–170.
728 <https://doi.org/10.1016/j.gca.2014.12.007>

729 Weyer, S., Anbar, A.D., Gerdes, A., Gordon, G.W., Algeo, T.J., Boyle, E.A., 2008. Natural
730 fractionation of $^{238}\text{U}/^{235}\text{U}$. *Geochim. Cosmochim. Acta* 72, 345-359.
731 <https://doi.org/10.1016/j.gca.2007.11.012>

732